J Biol Inorg Chem (2013) 18:137–144
DOI 10.1007/s00775-012-0958-0

ORIGINAL PAPER

Elucidating the mechanism of ferrocytochrome *c* heme disruption by peroxidized cardiolipin

Andrej Musatov · Marian Fabian · Rastislav Varhač

Received: 21 July 2012 / Accepted: 1 November 2012 / Published online: 18 November 2012

Abstract The interaction of peroxidized cardiolipin with ferrocytochrome *c* induces two kinetically and chemically distinct processes. The first is a rapid oxidation of ferrocytochrome *c*, followed by a slower, irreversible disruption of heme *c*. The oxidation of ferrocytochrome *c* by peroxidized cardiolipin is explained by a Fenton-type reaction. Heme scission is a consequence of the radical-mediated reactions initiated by the interaction of ferric heme iron with peroxidized cardiolipin. Simultaneously with the heme *c* disruption, generation of hydroxyl radical is detected by EPR spectroscopy using the spin trapping technique. The resulting apocytochrome *c* sediments as a heterogeneous mixture of high aggregates, as judged by sedimentation analysis. Both the oxidative process and the destructive process were suppressed by nonionic detergents and/or high ionic strength. The mechanism for generating radicals and heme rupture is presented.

A. Musatov · M. Fabian · R. Varhač
Department of Biochemistry, The University of Texas Health Science Center, San Antonio, TX 78229-3900, USA

Present Address:
A. Musatov (✉)
Institute of Experimental Physics Slovak Academy of Science, Watsonova 47, Kosice, Slovakia
e-mail: musatov@uthscsa.edu

M. Fabian
Department of Biochemistry and Cell Biology, Rice University, P.O. Box 1892, Houston, TX 77251-1892, USA

R. Varhač
Department of Biochemistry, Pavol Jozef Šáfarik University, Moyzesova 11, 04167 Kosice, Slovakia

Keywords Ferrocytochrome *c* · Peroxidized cardiolipin · Heme destruction · Hydroxyl radical · Aggregation

Abbreviations

CL	Cardiolipin
CLOOH	Peroxidized cardiolipin
cyt c^{2+}	Ferrocytochrome c
cyt c^{3+}	Ferricytochrome *c*
POBN	α-(4-Pyridyl-1-oxide)-*N*-*tert*-butyl nitrone
Tris	Tris(hydroxymethyl)aminomethane

Introduction

Cardiolipin (CL; 1,3-diphosphatidyl-*sn*-glycerol) is a unique phospholipid having four acyl groups and two negative charges. It is found exclusively in the inner mitochondrial membrane and bacterial plasma membranes. Two populations of CL exist within the inner mitochondrial membrane: the first CL population is tightly bound to mitochondrial inner-membrane proteins, such as cytochrome *c* oxidase [1, 2], the cytochrome bc_1 complex [3–5], complex I [4], ATP/ADP translocase [6], F_0F_1 ATP synthase [7], phosphate carrier [8], and succinate dehydrogenase [9]; the second CL population is not bound to proteins and is free to diffuse within the bilayer of the inner mitochondrial membrane. It is generally accepted that in addition to helping maintain the structural integrity of the inner mitochondrial membrane, the bilayer CL can also bind cytochrome *c*. CL contains a much higher ratio of unsaturated to saturated fatty acid residues than do other mitochondrial phospholipids (80–90 % linoleic acid); therefore, CL is much more susceptible to oxidative damage than mitochondrial phosphatidylcholine (1,2-dioleoyl-*sn*-glycero-3-phosphocholine) or phosphatidylethanolamine.

Cytochrome *c* is a small globular protein located in the mitochondrial intermembrane space, where its main function is to shuttle electrons from cytochrome bc_1 to cytochrome *c* oxidase during respiration. Cytochrome *c* also has catalase/peroxidase-like activity, which can be part of the mechanism protecting against oxidative damage in mitochondria [10]. The next line of defense against oxidative damage is the reactivity of cytochrome *c* with superoxide, which also has technological applications for the construction of biosensors [11]. In addition, cytochrome *c* has a significant role in the activation of programmed cell death. Release of cytochrome *c* from the mitochondria to the cytosol is a key step in the induction of the apoptotic cascade that leads to programmed cell death [12, 13]. The apoptotic activity of cytochrome *c* can also be controlled via interaction with antiapoptotic proteins [14]. In mitochondria, cytochrome *c* is bound to the inner membrane primarily by CL. Peroxidation of bilayer CL would be expected to generate a high local concentration of lipid peroxide near the cytochrome *c* binding site. Indeed, multiple studies point to the role of oxidative modification of CL resulting in loss of molecular interaction between CL and cytochrome *c*; however, the precise mechanism of this reaction is not known [15, 16].

In this study, we used absorption spectroscopy and EPR spectroscopy to probe the effect of oxidative modification of CL on its interaction with the reduced form of cytochrome *c* in vitro. The resulting modified protein was also analyzed by sedimentation velocity analysis. Our data reveal that the reaction of ferrocytochrome *c* (cyt c^{2+}) with peroxidized CL (CLOOH) of bovine origin results in a two-phase process: first, the oxidation of cyt c^{2+}, and second, heme *c* rupture. Moreover, in contrast to untreated protein or unmodified CL-treated cytochrome *c*, which sediments as a homogeneous species, CLOOH-treated cytochrome *c* sediments as a very heterogeneous mixture of high aggregates. The mechanism of the reaction of CLOOH with cyt c^{2+} is discussed.

Materials and methods

Materials

Bovine CL and phosphatidylcholine in chloroform or lyophilized were obtained from Avanti Polar Lipids. Dodecyl maltoside was from Anatrace. Horse heart cytochrome *c* (purity 95 % or greater), sodium dithionite, and hydrogen peroxide were from Sigma. The reduced form of cytochrome *c* was prepared with excess of sodium dithionite, followed by gel filtration (Sephadex PD-10, Amersham Biosciences). The concentrations of ferricytochrome *c* (cyt c^{3+}) and cyt c^{2+} were determined using ε_{410}(ox) $= 106\ \mathrm{mM^{-1}\ cm^{-1}}$ and ε_{550}(red) $= 27.7\ \mathrm{mM^{-1}\ cm^{-1}}$, respectively [17]. An α-(4-pyridyl-1-oxide)-*N*-*tert*-butyl nitrone (POBN) spin trap of high purity was obtained from Alexis Biochemicals. All other chemicals were reagent grade.

CL peroxidation

Commercially available CL was peroxidized essentially as reported by Parinandi et al. [18] with a minor modification. Briefly, CL in chloroform was dried under nitrogen and the resulting film was suspended by vortexing in 0.15 M NaCI, with the pH adjusted to 7.4 with $NaHCO_3$, for 3 min followed by sonication using a Branson model 250 sonifier. Finally, air was slowly blown through the resulting suspension at 25 °C for 2–4 h. To remove salt, CLOOH was extracted using chloroform/methanol/water [19], dried under nitrogen, and dissolved in chloroform. The extent of lipid peroxidation was determined by the generation of conjugated dienes as described by Buege and Aust [20] using $\varepsilon_{234} = 25.2\ \mathrm{mM^{-1}\ cm^{-1}}$. Visible spectra were collected using an SLM Aminco 3000 diode-array spectrophotometer.

Liposome preparation

The phospholipids in chloroform were dried under nitrogen, and the resulting film was suspended by vortexing in 20 mM tris(hydroxymethyl)aminomethane (Tris)–Cl, 1 mM EDTA buffer, pH 7.4. The mixture was clarified by sonication for a few minutes on ice under nitrogen using a Branson model 250 sonifier. Substitution of 20 mM phosphate buffer for 20 mM Tris–Cl buffer or omission of EDTA did not affect the results.

EPR spectroscopy

All EPR samples were prepared in 20 mM Tris–Cl buffer, pH 7.4. The reaction was initiated by the addition of CLOOH (167 μM) to a mixture of cyt c^{2+} (10 μM) with POBN (48 mM) and then the sample was transferred to a capillary tube for EPR measurements.

EPR spectra were recorded with a Varian E-6 spectrometer at 25 °C. The conditions for the measurements were as follows: modulation amplitude 1 G; microwave power 10 mW; frequency 9.225 GHz; time constant 1; and scan time 4 min.

Analytical ultracentrifugation

Sedimentation velocity studies were performed with a Beckman Optima XL-I analytical ultracentrifuge with a four-hole An-60 titanium rotor. All samples were analyzed

in 25 mM phosphate buffer, 1 mM EDTA pH 7.2 buffer with or without 25 μM CL or CLOOH after 30 min incubation at 25 °C. The rotor speed was 50,000 rpm. Data were collected at 25 °C using optical absorption detection at 280 nm. The resulting data were analyzed by the method of van Holde and Weischet [21] using the data analysis program UltraScan II version 9.3 developed by B. Demeler (Department of Biochemistry, University of Texas Health Sciences Center). The experimental data were corrected for buffer density and viscosity. The effect of CL density and viscosity, however, was not considered; therefore, the sedimentation values obtained for cytochrome *c* in the presence of CL micelles are presented as observed sedimentation coefficients.

Results

CLOOH-induced oxidation and disruption of heme *c*

A blueshifted Soret band and intensity decreases were observed immediately after mixing CLOOH with cyt c^{2+} (Fig. 1). The first spectrum recorded approximately 10 s following initiation of the reaction is characteristic of cyt c^{3+}. A comparison of the spectrum of cyt c^{3+} with the spectrum of cyt c^{2+} reacted with CLOOH for 10 s confirms that the two spectra are nearly identical. Such a CLOOH-generated form of cytochrome *c* is fully reducible by sodium ascorbate, suggesting that heme *c* remains intact.

Oxidation of cyt c^{2+} is followed by a slower disappearance of the heme *c* absorption (Fig. 1). For example, the Soret absorption band of 2.3 μM cyt c^{2+} decreased by about 83 % after incubation with 25 μM CLOOH for 30 min at 25 °C (Fig. 1c). Addition of sodium ascorbate to CLOOH-treated cytochrome *c* (for more than 10 s) does not restore a Soret maximum at 414 nm, suggesting an irreversible loss of heme *c* reducibility (Fig. 2). The extent of heme *c* destruction was time- and concentration-dependent. Oxidation of heme *c* and heme *c* rupture were also observed if cyt c^{2+} was added to CLOOH–1,2-dioleoyl-*sn*-glycero-3-phosphocholine liposomes (1:1 w/w); however, the extent of heme *c* disruption was about 30 % lower than in the case of pure CLOOH micelles. Without CL or CLOOH, cyt c^{2+} is stable in solution. With or without detergent and/or salt, it did not show measurably altered visible absorption spectra for at least 30 min at 25 °C.

To establish if the disruption of heme *c* is affected by the redox state of cytochrome *c*, the reactions of CLOOH with cyt c^{2+} and cyt c^{3+} were compared. Under identical

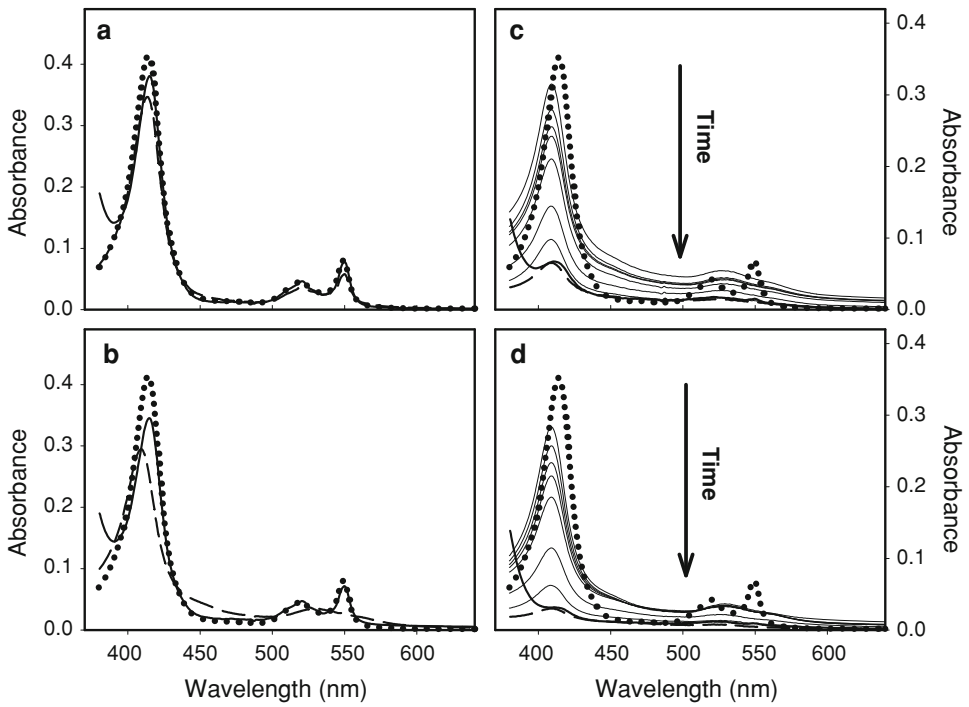

Fig. 1 Concentration- and time-dependent effect of peroxidized cardiolipin (CLOOH) on ferrocytochrome *c* heme disruption. Absolute spectra of ferrocytochrome *c* were taken before incubation (*dotted lines*), after incubation with CLOOH for 30 min at room temperature (*dashed lines*), and after addition of 5 mM sodium ascorbate (*thick solid lines*). **c**, **d** Spectra taken 0.25, 1, 2, 3, 5, 10, and 15 min after addition of CLOOH to ferrocytochrome *c* (*thin black lines*). The initial concentrations of ferrocytochrome *c* were 2.9 μM (**a**, **b**) and 2.3 μM (**c**, **d**). The concentrations of CLOOH were 5, 10, 25, and 50 μM in **a**, **b**, **c**, and **d**, respectively. Baselines were taken for CLOOH in 20 mM tris(hydroxymethyl)aminomethane (Tris)–Cl, 1 mM EDTA buffer, pH 7.4

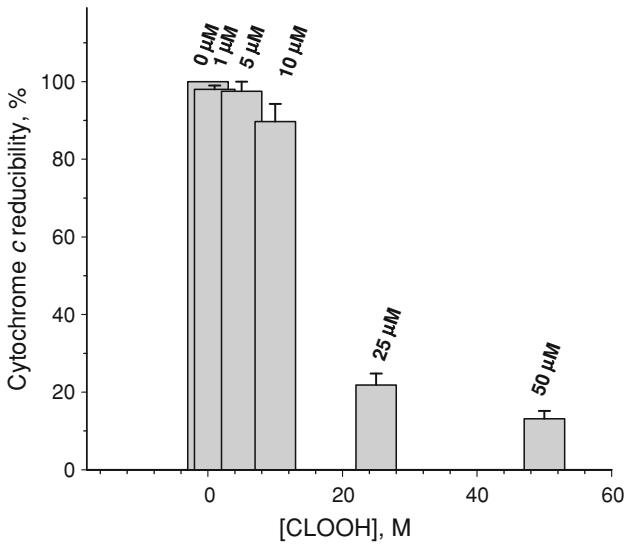

Fig. 2 Reducibility of CLOOH-treated ferrocytochrome *c*. Ferrocytochrome *c* was treated with 0, 1, 5, 10, 25, or 50 μM CLOOH for 30 min at 25 °C. After incubation of ferrocytochrome *c* with CLOOH for 30 min at 25 °C, the reducibility of heme *c* was determined from the optical spectra with addition of 5 mM sodium ascorbate using ε_{550}(red–ox) = 21 mM^{-1} cm^{-1}

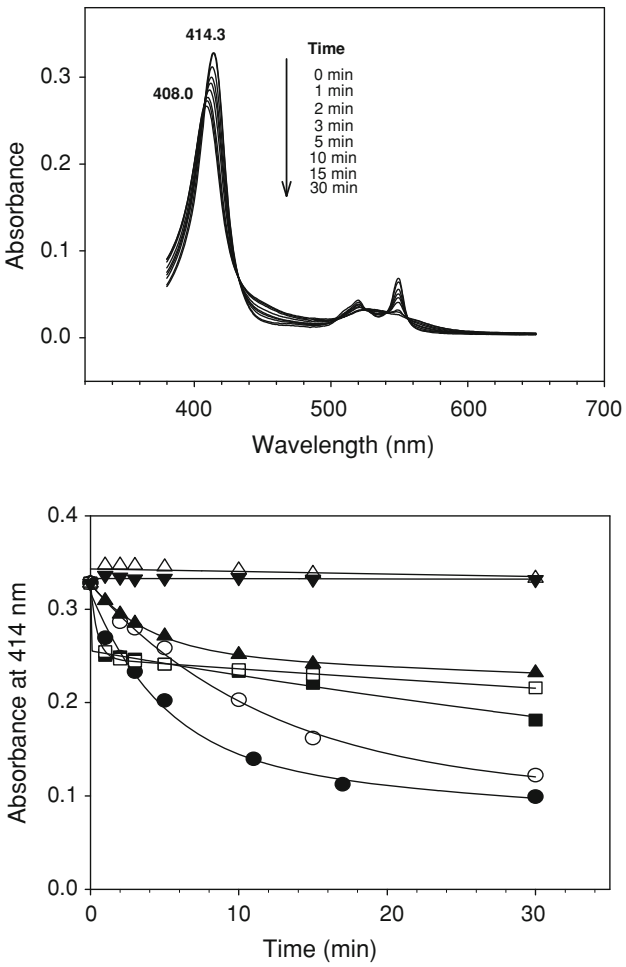

Fig. 3 Ionic-strength-dependent spectral changes of ferrocytochrome *c* in the presence of CLOOH. *Upper panel*: Time-dependent spectral changes of 2.5 μM ferrocytochrome *c* reacted with 25 μM CLOOH in 20 mM Tris–Cl buffer pH 7.4, containing 1 mM EDTA and 150 mM NaCl. *Lower panel*: Ionic-strength-dependent and time-dependent changes of absorbance monitored at 414 nm during the interaction of cytochrome *c* (2.5 μM) with CLOOH (25 μM) in the absence of NaCl (*solid circles*) and in the presence of various concentrations of NaCl: 20 mM (*open circles*), 60 mM (*solid squares*), 100 mM (*open squares*), 150 mM (*solid upward triangles*), 500 mM (*open upward triangles*), and 1 M (*inverted triangles*)

experimental conditions, the reactions did not differ in either the rate or the amount of heme *c* destroyed (data not shown).

The extent of heme *c* destruction was affected by oxygen. When reaction of 9.5 μM cyt c^{2+} with 100 μM CLOOH was performed in argon-saturated buffer, the extent of heme *c* degradation increased but the rate of degradation ($k = 0.014$ s^{-1}) was unchanged compared with that for the reaction in air-saturated buffer (data not shown).

Both CLOOH-induced oxidation and heme *c* disruption were completely prevented if the same experiments were performed in the presence of 2 mM nonionic detergent, such as dodecyl maltoside, Triton X-100, or Tween-20, suggesting solubilization of CL liposomes, formation of detergent–CL micelles, and elimination of CL–cyt c^{2+} hydrophobic interaction. In addition, the interaction of CLOOH with cyt c^{2+} was dependent on the ionic strength. When cyt c^{2+} and CLOOH-containing vesicles were mixed in buffers with increased NaCl concentration (20–150 mM), CLOOH-initiated heme *c* rupture disappeared, although oxidation of cyt c^{2+} was still observed. Complete inhibition of oxidation and degradation of heme *c* was achieved at an NaCl concentration greater than 0.5 M (Fig. 3).

Reaction of unmodified CL with cyt c^{2+} at neutral pH produces changes in the absorption spectrum in the Soret region similar to those described previously [22–24] and explained by either oxidation of cyt c^{2+} due to generation of a monoepoxide of linoleic acid [22] or conformational changes of cytochrome *c* [24]. The Soret maximum of cyt c^{2+} was blueshifted from an initial value of 414.0–410.5 nm after 30 min incubation with 25 μM CL. The maximum absorbance in the Soret region decreased by about 10 %. A decrease in intensity was also observed at 550 nm. Changes in both the absolute spectrum and the difference spectrum indicate the oxidation of cyt c^{2+}. The spectral changes were fully reversible. Addition of 5 mM sodium ascorbate resulted in complete recovery of the initial absolute spectrum of reduced cytochrome *c*.

Kinetic analysis and EPR spectroscopy study of the reaction of CLOOH with cyt c^{2+}

Upon mixing reduced cytochrome *c* with CLOOH, the protein is oxidized in less than 10 s. Oxidation is followed by the disappearance of heme absorption (Fig. 4b). The loss of heme absorption occurs in two phases described by rate constants $k_1 = 8 \times 10^{-3}$ s^{-1} (contribution 83 %) and $k_2 = 2 \times 10^{-4}$ s^{-1} (17 %). Simultaneously with heme *c* destruction, observed by absorption spectroscopy, radical formation was detected using POBN spin trap EPR spectroscopy. The EPR spectra clearly exhibit rising and falling phases of POBN adduct formation within the time of observation (Fig. 4a). The fit of the dependence of the EPR amplitude indicates that the rate of the rising phase is very close to that for the fast phase of loss of absorption of heme (Fig. 4b). Both occur with rates of approximetly 8×10^{-3} s^{-1}.

A six-line EPR spectrum results from hyperfine coupling of nitrogen, $A_N = 14.5$ G, and hydrogen, $A_H = 1.5$ G (Fig. 4a). The magnitudes of these splittings are not identical but are close to values for the adduct of OH· and POBN in benzene, where the corresponding splittings were 14.5 and 1.8 [25]. In the more polar solvent water, the values for nitrogen are larger, with values between 14.93 and 14.97. However, A_H in water is decreased to 1.68 [25]. This imperfect fit of observed spin adduct parameters with the tabulated data can be reconciled by the assumption that the adduct of OH· and POBN is located in the hydrophobic core of CLOOH vesicles. In control EPR measurements performed on pure POBN (58 mM), reduced cytochrome *c* (10 μM) with POBN (58 mM), and CLOOH (167 μM) with POBN (48 mM) the EPR signal was not observed or developed (data not shown).

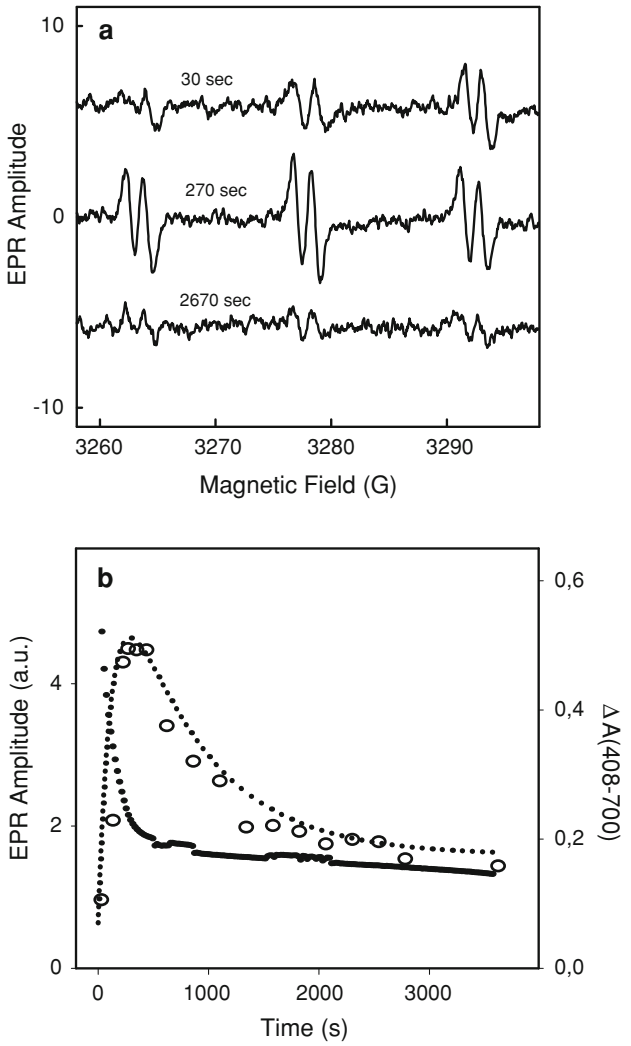

Fig. 4 EPR spectra and kinetics of formation of α-(4-pyridyl-1-oxide)-*N-tert*-butyl nitrone (POBN) radical adducts during reaction of reduced cytochrome *c* with CLOOH. **a** The EPR spectra following the reaction of 8.3 μM reduced cytochrome *c* and 167 μM CLOOH in the presence of 48 mM spin trap POBN. Spectra were continually collected with a scan time of 4 min at 25 °C. Recording was started 30, 270, and 2,670 s following the addition of CLOOH to the sample. **b** The dependencies of the EPR amplitude of the single line (*open circles*) and the optical absorbance at the Soret band (*solid circles*) on the reaction time. Optical measurements were performed using the same concentrations as those in the EPR measurements, but without the spin trap. *Circles* experimental data, *dotted line* two-exponential fit

Apoprotein aggregation

Cyt c^{2+} in low ionic strength buffer sediments as a monodisperse homogeneous species with $s_{20,W}$ of 1.8 S (Fig. 5). The homogenous sedimentation behavior of cytochrome *c* was unaffected by treatment of the protein with unmodified CL. However, cytochrome *c* was a very heterogeneous

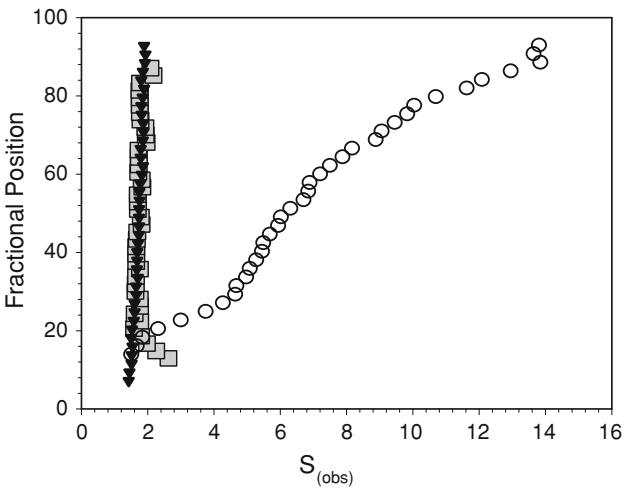

Fig. 5 Aggregation of CLOOH-treated ferrocytochrome *c* analyzed by sedimentation velocity. The ferrocytochrome *c* aggregation state was analyzed after 30 min incubation at 25 °C in 25 mM phosphate buffer, 1 mM EDTA pH 7.2 buffer containing no additions (*triangles*), containing 25 μM cardiolipin (*squares*), or containing 25 μM CLOOH (*circles*)

mixture of high molecular weight aggregates when the sedimentation velocity analysis was performed after reaction with CLOOH. Observed sedimentation coefficients ranged from 1.8 to 15 S, indicating aggregation of protein.

Discussion

The reaction of cyt c^{2+} with CLOOH was examined using absorption spectroscopy, EPR spectroscopy, and sedimentation velocity analysis. In the presence of CLOOH, cyt c^{2+} is oxidized, with subsequent destruction of heme *c*.

Oxidation of cyt c^{2+} and scission of the heme ring

The initial rapid oxidation of CLOOH-reacted cyt c^{2+} is implicated by both the spectroscopic analysis and kinetic data. Two lines of evidence suggest that the form of cytochrome *c* obtained is indeed oxidized protein. The first evidence is the optical spectrum of cytochrome *c* exposed briefly (approximately 10 s) to CLOOH. This spectrum is nearly identical to that of the native untreated cyt c^{3+}. Also the presence of the charge transfer band at approximately 700 nm characteristic of cyt c^{3+} indicates the presence of unmodified six-coordination ferric iron following brief exposure to CLOOH (data not shown). Additionally, this exposed cytochrome *c* is fully reducible by either sodium ascorbate or sodium dithionite.

Second, evidence supporting the initial formation of oxidized cytochrome *c* as a result of reaction with CLOOH that is equivalent to the native ferric protein comes from a comparison of the rates of heme destruction. Under the same experimental conditions, both the rates and the final amount of damaged heme were identical in the reactions of native cyt c^{3+} and cyt c^{2+} with CLOOH. If the oxidized protein produced at the beginning of the interaction of cyt c^{2+} with CLOOH were not identical to the native cyt c^{3+}, then the rates of heme degradation would have shown some disparity. However, this is not the case, and both forms of cytochrome *c* displayed equal reactivity towards CLOOH.

The cleavage of heme *c* induced by CLOOH is demonstrated by the irreversible loss of the UV–vis absorption of the protein and by significant changes in the protein aggregation state. The absence of heme *c* degradation in experiments when cyt c^{2+} reacts with unmodified CL indicates the initiation of the reaction by CLOOH.

The interaction of CLOOH with cyt c^{2+} results in the generation of hydroxyl radicals (OH·) as demonstrated by the EPR data. Both EPR and absorption spectroscopy kinetic data indicate that the effect of CLOOH on cyt c^{2+} consists of two stages: a rapid oxidation of cyt c^{2+} followed by a slower biphasic destruction of cyt c^{3+}, described by the two rate constants. The oxidation of cyt c^{2+} by CLOOH can be explained by a Fenton-type reaction [26]:

$$\text{Cyt}\,c - \text{Fe}^{2+} + \text{CLOOH} \rightarrow \text{Cyt}\,c - \text{Fe}^{3+} + \text{CLO}^{-} + \text{OH}\cdot$$

Unfortunately, the hydroxyl radicals produced by this reaction were not detected by EPR spectroscopy since the first EPR data were acquired 30 s after initiation of the reaction, making detection of the short-lived hydroxyl radical impossible. It is reasonable to assume that as soon as hydroxyl radicals are generated by the Fenton reaction, they immediately attack the oxidized heme *c*, resulting in heme disruption, which is accompanied by the release of non-heme Fe^{3+}. Therefore, hydroxyl radicals detected by EPR spectroscopy are most likely generated by the Haber–Weiss mechanism using released Fe^{3+} as a catalyst [27]:

$$\text{CLOOH} + \text{OH}\cdot \rightarrow \text{CLOH} + \text{O}_2^{\cdot -} + \text{H}^{+}$$

$$\text{O}_2^{\cdot -} + \text{Fe}^{3+} \rightarrow \text{Fe}^{2+} + \text{O}_2$$

$$\text{CLOOH} + \text{Fe}^{2+} \rightarrow \text{Fe}^{3+} + \text{CLO}^{-} + \text{OH}\cdot$$

Good correlation of the rates of hydroxyl radical production and the first phase of heme *c* rupture ($k_1 = 8 \times 10^{-3}\ \text{s}^{-1}$) suggests that hydroxyl radicals are mostly responsible for heme destruction. Hydroxyl radical generation and, therefore, heme *c* destruction, were also registered during the second, slower phase with $k_2 = 2 \times 10^{-4}\ \text{s}^{-1}$. The question, however, remains whether hydroxyl- radical-induced damage is the only mechanism of heme *c* rupture. An additional and plausible mechanism of heme *c* degradation is based on generation of ferryl iron and either an alkoxyl or a peroxyl radical:

$$\text{Fe}^{3+} + \text{CLOOH} \rightarrow \text{CLO}\cdot + \text{OH}^{-} + \text{Fe}^{4+}$$

CLO· radicals are further involved in the release of OH· by the reaction

$$\text{CLO}\cdot + \text{CLOOH} \rightarrow \text{CL} - \text{O} - \text{O} - \text{CL} + \text{OH}\cdot$$

The generation of an alkoxyl or a peroxyl radical during the reaction of fatty acids with heme proteins and their destructive effect is well known [28–32]. Moreover, similar mechanisms, based on formation of Fe^{4+} (Fe^{5+}) forms, have been proposed for destruction of heme *c* by *tert*-butyl hydroperoxide [33] and degradation of cytochrome P450 [32].

The enhancement of heme degradation in the presence of O_2 can be understood on the basis of propagation of peroxidation of lipids by radicals:

$$\text{CLO}\cdot + \text{CL} - \text{H} \rightarrow \text{CL} - \text{OH} + \text{CL}\cdot$$

$$\text{CL}\cdot + \text{O}_2 \rightarrow \text{CL} - \text{O} - \text{O}\cdot$$

$$\text{CL} - \text{O} - \text{O}\cdot + \text{CL} - \text{H} \rightarrow \text{CL} - \text{O} - \text{O} - \text{H} + \text{CL}\cdot$$

The reactions above lead to the increase in concentration of hydroperoxides that further promote heme scission to a

larger extent than that occurring under anaerobic conditions.

Neither sodium ascorbate nor sodium dithionite can reduce the CLOOH-modified cytochrome *c*. CLOOH is effective even at very low concentrations. Nearly 80–90 % of heme *c* destruction occurs with a molar ratio of CLOOH to cyt c^{2+} of 10–20. These concentrations of CLOOH are approximately 100 times lower than the concentrations of *tert*-butyl hydroperoxide that is required to bleach cyt c^{3+} to a similar extent [34].

The reaction of CLOOH with cyt c^{2+} is in sharp contrast with the effect of H_2O_2 on cyt c^{2+}. Reaction of cyt c^{2+} with 5–100 μM H_2O_2 is characterized by a very slow rate of heme *c* oxidation, with no evidence of heme *c* destruction. For example, treatment of 3.5 μM cyt c^{2+} with 50 μM H_2O_2 for 30 min resulted in a less than 5–7 % decrease of absorbance in the α and γ spectral bands, which was fully reversible by addition of sodium ascorbate (data not shown).

The effectiveness of CLOOH can be explained by the exceptionally specific nature of interaction with cytochrome *c*. According to the extended lipid conformational model [35], one acyl chain of CL penetrates into the hydrophobic channel of cytochrome *c*; therefore, in the case of CLOOH, a peroxy group would be localized close to heme *c* (Fig. 6). Moreover, a recent model of the cytochrome *c*–CL complex suggests the insertion of two acyl chains of CL into the hydrophobic channel of the same cytochrome *c* molecule [36].

Binding of unmodified CL involves both hydrophobic and ionic interactions [35, 37–40]. Oxidatively modified CL is also capable of binding to cytochrome *c*, although the binding is not as strong as with nonoxidized CL [41, 42]. Our data also suggest that the binding of CLOOH to cyt c^{2+} involves both hydrophobic and ionic interactions. Addition of detergent or increase of ionic strength results in a decrease or elimination of the effect of CLOOH on cyt c^{2+}. The significance of a hydrophobic interaction has been stressed by Kapetanaki et al. [43], who found that addition of the nonionic detergent Triton X-100 completely abolished the interaction of carbon monoxide with the cyt c^{2+}–CL complex. CLOOH-induced inhibition of both oxidation and heme *c* bleaching by nonionic detergents is very likely due to solubilization of lipid vesicles. This solubilization results in the dispersion of CL into the small detergent micelles. We assume that in these mixed micelles CL is thermodynamically stabler relative to the pure CL vesicles. The relative stabilization or stronger binding of CL in lipid–detergent micelles may be a reason for the inability of lipid to reach the hydrophobic pocket of cytochrome *c* and to initiate the oxidative/bleaching reactions. The stabilization of CL in micelles may have its origin in the change of the energy of interaction between acyl chains, in the change of the electrostatic repulsion between negatively charged CL polar heads, or in the combination of both of these factors. Clearly, we can expect that in micelles, having a smaller radius than lipid vesicles, the distance between the charged CL heads should be increased. Consequently, the electrostatic repulsion between the heads of CL is decreased and the stability of lipids in micellar aggregates should be enhanced. Our results also agree with the observation that unmodified CL triggers spectral changes within cyt c^{2+} [22–24] reflecting the oxidation of reduced cytochrome *c* (see "Results").

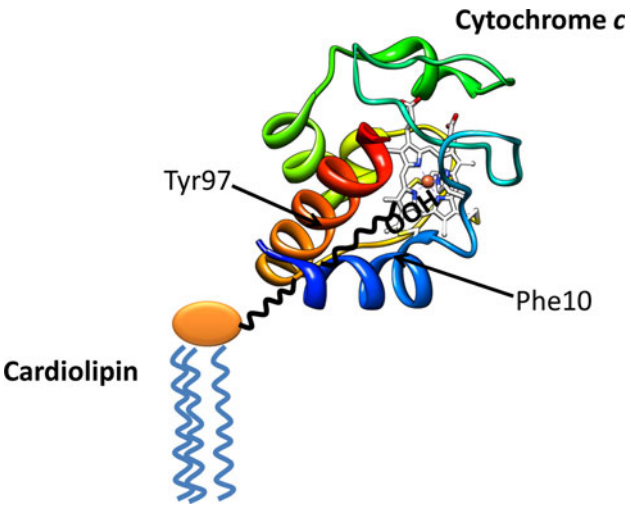

Fig. 6 Model of the cytochrome *c*–CLOOH complex. Insertion of a monohydroperoxide cardiolipin acyl chain (*black*) into the hydrophobic pocket of cytochrome *c* surrounded by Tyr97 and Phe10. The heme is in *white*, and the iron ion is shown as a *dark-orange sphere*. The protein structure was visualized with Protein Data Bank entry 1CRC

The possible effect of CL polymorphism or structural reorganization of CL in aqueous solvents should also be considered. Pure CL or CL–phospholipid mixtures in aqueous solvents are organized in typical unilamellar liposomes [44]. However, under certain conditions, CL is capable of forming the inverted hexagonal phase (H_{II}) [45, 46]. For example, Ca^{2+}, Mg^{2+}, and Ba^{2+} salts induce well-defined bilayer–hexagonal (H_{II}) transitions [47] More importantly, this transition can be also triggered by cytochrome *c* [48]. Therefore, in addition to structural alterations of cytochrome *c*, it is likely that concurrent perturbation of CL liposomes can facilitate the interaction between the acyl chain of lipids and the hydrophobic pocket of cyt c^{2+}.

Heme *c* degradation also caused significant changes in the aggregation state of cytochrome *c*. Cyt c^{2+} before or after exposure to unmodified CL sediments as homogeneous species (sedimentation coefficient of about 1.8 S). However, when cyt c^{2+} is reacted with CLOOH, it sediments as highly heterogeneous species with sedimentation

coefficients ranging from 1.8 to 15 S. The aggregation of cytochrome *c* is most likely initiated by exposure of hydrophobic sites on cytochrome *c* by the radical-induced formation of cross-links between the individual proteins.

In conclusion, our results demonstrate that CLOOH rapidly oxidizes cyt c^{2+}, followed by a slower biphasic degradation of heme *c* together with aggregation of the protein. Although these results were obtained in vitro, we envisage that such effects are relevant to in vivo exposure of cytochrome *c* to CLOOH in mitochondria, although this assumption remains to be examined.

Acknowledgments This work was supported by grants from the National Institutes of Health (NIH GM024795 for Neal C. Robinson and NIH GM0843348 for M.F.) and from the European Union Structural Fund (ESF 26110230061). Sedimentation velocity analyses were performed in the Center for Analytical Ultracentrifugation of Macromolecular Assemblies of the University of Texas Health Science Center at San Antonio. The authors thank Virgil Schirf for technical assistance. The authors also thank Neal C. Robinson (University of Texas Health Science Center at San Antonio) for his invaluable discussions regarding these data and for editorial help in preparing the manuscript.

References

1. Sedlák E, Robinson NC (1999) Biochemistry 38:14966–14972
2. Robinson NC (1993) J Bioenerg Biomembr 25:153–163
3. Gomez B Jr, Robinson NC (1999) Biochemistry 38:9031–9038
4. Fry M, Green DE (1981) J Biol Chem 256:1874–1880
5. Lange C, Nett JH, Trumpower BL, Hunte C (2001) EMBO J 20:6591–6600
6. Beyer K, Klingenberg M (1985) Biochemistry 24:3821–3826
7. Eble KS, Coleman WB, Hantgan RR, Cunningham CC (1990) J Biol Chem 265:19434–19440
8. Kadenbach B, Mende P, Kolbe HV, Stipani I, Palmieri F (1982) FEBS Lett 139:109–112
9. Yankovskaya V, Horsefield R, Tornroth S, Luna-Chavez C, Miyoshi H, Leger C, Byrne B, Cecchini G, Iwata S (2003) Science 299:700–704
10. Sedlák E, Fabian M, Robinson NC, Musatov A (2010) Free Radic Biol Med 49:1574–1581
11. Wegerich F, Turano P, Allegrozzi M, Mohwald H, Lisdat F (2009) Anal Chem 81:2974–2984
12. McMillin JB, Dowhan W (2002) Biochem Biophys Acta 1585:97–107
13. Ott M, Robertson JD, Zhivotovsky B, Orrenius S (2002) Proc Natl Acad Sci USA 99:1259–1263
14. Bertini I, Chevance S, Del Conte R, Lalli D, Turano P (2011) PLoS ONE 6(4):e18329. doi:10.1371/journal.pone.0018329
15. Kagan VE, Tyurin VA, Jiang J, Tyurina YY, Ritov VB, Amoscato AA, Osipov AN, Belikova NA, Kapralov AA, Kini V, Vlasova II, Zhao Q, Zou M, Di P, Svistunenko DA, Kurnikov IV, Borisenko GG (2005) Nat Chem Biol 1:223–232
16. Petrosillo G, Ruggiero FM, Pistolese M, Paradies G (2001) FEBS Lett 509:435–438
17. Margoliash E, Frohwirt N (1959) Biochem J 71:570–572
18. Parinandi NL, Weis BK, Schmid HH (1988) Chem Phys Lipids 49:215–220
19. Bligh EG, Dyer WJ (1959) Can J Biochem Physiol 37:911–917
20. Buege JA, Aust SD (1978) Methods Enzymol 52:302–310
21. van Holde KE, Weischet WO (1978) Biopolymers 17:1387–1403
22. Iwase H, Takatori T, Nagao M, Iwadate K, Nakajima M (1996) Biochem Biophys Res Commun 222:83–89
23. Tuominen EKJ, Wallace CJA, Kinnunen PKJ (2002) J Biol Chem 277:8822–8826
24. Nantes IL, Zucchi MR, Nascimento OR, Faljoni-Alario A (2001) J Biol Chem 276:153–158
25. Buetner GR (1987) Free Radic Biol Med 3:259–303
26. Fenton HJH (1894) J Chem Soc 65:899–909
27. Haber F, Weiss J (1934) Proc R Soc Lond 147:332–351
28. Aft RL, Mueller GC (1984) J Biol Chem 259:301–305
29. Gutteridge JM, Smith A (1988) Biochem J 256:861–865
30. Rota C, Barr DP, Martin MV, Guengerich FP, Tomasi A, Mason RP (1997) Biochem J 328:565–571
31. Dix TA, Marnett LJ (1985) J Biol Chem 260:5351–5357
32. Nagababu E, Rifkind JM (2004) Antioxid Redox Signal 6:967–978
33. Nantes IL, Faljoni-Alário A, Nascimento OR, Bandy B, Gatti R, Bechara EJH (2000) Free Radic Biol Med 28:786–796
34. Cadenas E, Boveris A, Chance B (1980) Biochem J 187:131–140
35. Rytömaa M, Kinnunen PKJ (1995) J Biol Chem 270:3197–3202
36. Sinibaldi F, Howes BD, Piro MC, Polticelli F, Bombelli C, Ferri T, Coletta M, Smulevich G, Santucci V (2010) J Biol Inorg Chem 15:689–700
37. Nichols P (1974) Biochim Biophys Acta 346:261–310
38. Cortese JD, Voglino AL, Hackenbrock CR (1998) Biochemistry 37:6402–6409
39. Gorbenko GP (1999) Biochim Biophys Acta 1420:1–13
40. Kalanxhi E, Wallace CJA (2007) Biochem J. 407:179–187
41. Shidoji Y, Hayashi K, Komura N, Ohishi N, Yagi K (1999) Biochem Biophys Res Commun 264:343–347
42. Nakagawa Y (2004) Ann N Y Acad Sci 1011:177–184
43. Kapetanaki SM, Silkstone G, Husu I, Liebl U, Wilson MT, Vos MH (2009) Biochemistry 48:1613–1619
44. Tarahovsky YS, Arsenault AL, MacDonald RC, McIntosh TJ, Epand RM (2000) Biophys J 79:3193–3200
45. De Kruijff B, Verkley AJ, Van Echteld CJA, Gerritsen WJ, Mombers C, Noordam PC, De Gier J (1979) Biochim Biophys Acta 555:200–209
46. Perutková Š, Daniel M, Dolinar G, Rappolt M, Kralj-Iglič V, Iglič A (2009) In: Leitmannova Liu A, Tien HT (eds) Advances in planar lipid bilayers and liposomes, vol 9. Academic, Burlington, pp 237–278
47. Vasilenko IB, De Kruijff B, Verkleij AJ (1982) Biochim Biophys Acta 684:282–286
48. De Kruijff B, Cullis PR (1980) Biochim Biophys Acta 602:477–490